Gayaz S. Khakimzyanov*, Oleg I. Gusev, Sofya A. Beizel, Leonid B. Chubarov, and Nina Yu. Shokina

Simulation of tsunami waves generated by submarine landslides in the Black Sea

Abstract: Numerical technique for studying surface waves appearing under the motion of a submarine landslide is discussed. This technique is based on the application of the model of a quasi-deformable landslide and two shallow water models, namely, the classic (dispersion free) one and the completely nonlinear dispersive model of the second hydrodynamic approximation. Numerical simulation of surface waves generated by a large model landslide on the continental slope of the Black Sea near the Russian coast is performed. It is shown that the dispersion has a significant impact on the picture of propagation of tsunami waves on sufficiently long paths.

Keywords: The Black Sea, submarine landslide, tsunami waves, dispersion, numerical algorithm.

MSC 2010: 76B15

DOI: 10.1515/rnam-2015-0020
Received February 19, 2015; accepted May 25, 2015

The water area of the Black Sea is specific for its high seismic activity [37] and is exposed to potential risk of tsunami waves [43, 49] generated not only by strong earthquakes, but also by submarine landslides [45] that may be caused by even weak seismic events. Bottom sediments sometimes lose their strength and begin movement over an underwater slope even without the impact of any earthquake [1, 24, 38].

Geophysical and hydrographic studies of the continental slope of the Black Sea show [10] that its large part is exposed to effects of submarine landslides and hence the waves generated in this process should be taken into account in risk estimation in the densely populated Black Sea coast, as well as for submarine pipelines intended to oil and gas transportation. The authors of [38] explain the anomalous fluctuations of the Black Sea level occurred at the Bulgarian coast on May 7, 2007 by just the landslide mechanism of surface waves generation.

Under the lack of data on the parameters of bottom sediments, the only source of some quantitative information about the wave processes arising in the case of potential submarine landslides is a computational experiment. The results of numerical simulation of landslide processes can be used in the design of engineering structures on the shelf and the continental slope, and also in evaluation of tsunami risk in particular areas of the coast.

In numerical experiments, a landslide is usually represented either as a rigid body moving over a flat slope [8, 9, 18, 48], or as a certain volume of near bottom fluid differing from water by a greater density [5, 14], or as a motion of some elasto-plastic medium [15]. In some papers (see, e.g., [24]) the motion of landslide was not modelled, but the surface waves generated by a landslide in its initial stage of motion were determined from empirical formulas derived on the base of numerous numerical and field studies [17]. The free surface obtained by empirical formulas was taken as an initial condition for calculation of surface waves under the assumption that the fluid under the initial wave was in its rest state. However, we have to note that the empirical formulas used in this case are valid only for the model of rigid landslide motion over a flat slope. The numerical experiments [4] have shown that the motion of a landslide over an uneven bottom results in a quite another picture of generated surface waves. Therefore, the simulation of real situations has to take into account [32] the roughness of the underwater slope and the probability of landslide deformation, as this was

***Corresponding Author: Gayaz S. Khakimzyanov:** Institute of Computational Technologies, Siberian Branch of the RAS, Novosibirsk 630090, Russia. E-mail: khak@ict.nsc.ru
Oleg I. Gusev, Sofya A. Beizel, Leonid B. Chubarov, Nina Yu. Shokina: Institute of Computational Technologies, Siberian Branch of the RAS, Novosibirsk 630090, Russia

done, for example, in experimental paper [31] where the deformation of a model landslide in its motion over an uneven surface was achieved due to its representation in the form of four rigid blocks sequentially linked by flexible connections. A similar technique was used in numerical simulation [38] with representation of a landslide as a finite set of blocks [46].

In this paper we use the model of quasi-deformable landslide [3], the equation of its motion was derived with partitioning its volume into infinite number of blocks, and the force moving it over the slope was taken as the sum of gravity, buoyancy, friction, and water resistance forces acting on infinitely small elementary volumes. Within this model, the form of landslide surface is changed according to unevenness of the bottom relief appearing in the course of motion (as for a deformable body), but the instant horizontal components of the velocity vector are the same at each point of the landslide (as for a rigid body). The appropriateness of the model is confirmed by the results of numerical studies of the specific nature of wave modes generated by the landslide near the Papua New Guinea coast on June 17, 1998.

Numerical studies of surface waves appearing in the motion of a submarine landslide were carried out with the use of the nonlinear dispersive (NLD) shallow water model from [13] because, in contrast with generally used NLD-models [24, 36, 47], it is invariant relative to the Galilean transformation and has a total energy balance equations coordinated with the three-dimensional Euler model. In some papers (see, e.g., [1]), the simulation of actual events was performed within the classic (dispersion free) shallow water model (NLSW-model). The simulation of the same events on the base of NLD-models often leads to ambiguous conclusions. For example, in paper [24] presenting numerical modelling of the landslide tsunami occurring on October 16, 1979 near Nice, the authors indicated that the use of wave dispersion gives the results practically identical to those obtained from a simpler NLSW-model. Other papers (see, e.g., [16, 33, 45]) indicate that dispersive effects essentially affect the process of wave propagation especially in their lasting movement. Our researches [6, 40, 41] for model water areas of simple geometry have shown that, in contrast to NLSW-models, the use of NLD-models always demonstrates the appearance of systems of dispersing waves and NLD-models satisfactorily describe a greater number of generated landslide waves than a dispersion free shallow water model.

This paper continues the studies related to the influence of the dispersion on the picture of surface waves generated by a landslide. In contrast with [40], here we consider landslides in the real Black Sea water area on high-resolution grids. NLD-equations are solved by a splitting method reducing the original problem to two more simple ones, namely, to a system of hyperbolic type equations and a scalar elliptic equation for the dispersive component of the pressure averaged over depth. Some results of calculations performed with the use of the NLD-model are presented. The comparison of these results with those obtained by a dispersion free shallow water model allows us to evaluate the importance of dispersive effects at the initial stage of wave generation by a submarine landslide in the process of their propagation in the deep-waver area and when they enter the coastal shelf.

1 Shallow water models and numerical algorithms

We use the Cartesian coordinate system $Oxyz$, the axis Oz is directed vertically up and the coordinate plane Oxy coincides with the horizontal unperturbed free surface of a layer of a perfect incompressible fluid bounded from below by a movable bottom given by the function $z = -h(x, y, t)$ and from above by a free boundary $z = \eta(x, y, t)$, where t is the time variable.

In shallow water models, the required values are the total depth $H = \eta + h > 0$ of the fluid layer and the velocity vector $\boldsymbol{u} = (u, v)$. In this paper we use models of the first and the second hydrodynamic approximation where $\boldsymbol{u}(x, y, t)$ is the horizontal component of the three-dimensional flow velocity vector averaged over the depth of the layer. The shallow water equations have the following form [13]:

$$H_t + \nabla \cdot (H\boldsymbol{u}) = 0 \tag{1.1}$$

$$(H\boldsymbol{u})_t + \nabla \cdot (H\boldsymbol{u}\boldsymbol{u}) + \nabla p = P_b \nabla h \tag{1.2}$$

where $\nabla = \left(\partial/\partial x,\ \partial/\partial y\right)$, $p = p(x, y, t)$ is obtained by integration of the pressure $P = P(x, y, z, t)$ over the depth of the layer, $P_b(x, y, t)$ is the pressure at the bottom.

The dispersion free NLSW-model uses the hydrostatic law of pressure variation $P = g(\eta - z)$, therefore,

$$p = \frac{gH^2}{2}, \quad P_b = gH.$$

Here $g = \text{const}$ is the acceleration of gravity. In the totally nonlinear NLD-model with dispersion the pressure P is [11] a quadratic function of the vertical coordinate z, i.e.,

$$P(z) = g(\eta - z) - (\eta - z) D^2 h - \left(\frac{H^2}{2} - \frac{(z+h)^2}{2}\right)\left[D(\nabla \cdot \boldsymbol{u}) - (\nabla \cdot \boldsymbol{u})^2\right].$$

Therefore,

$$p = \frac{gH^2}{2} - \varphi, \quad P_b = gH - \frac{1}{r}\left(\frac{6\varphi}{H} + HR + \nabla\varphi \cdot \nabla h\right)$$

where

$$R = -g\nabla\eta \cdot \nabla h + \boldsymbol{u} \cdot \left((\boldsymbol{u} \cdot \nabla)\nabla h\right) + h_{tt} + 2(\boldsymbol{u} \cdot \nabla h_t), \quad r = 4 + |\nabla h|^2$$

while φ is the dispersive component of the integrated pressure p,

$$\varphi = \frac{H^3}{3}\left[D(\nabla \cdot \boldsymbol{u}) - (\nabla \cdot \boldsymbol{u})^2\right] + \frac{H^2}{2} D^2 h$$

and $D = \partial/\partial t + \boldsymbol{u} \cdot \nabla$ is the total derivative operator.

We note that in comparison with the nonlinear dispersive equations proposed in [36, 47] for simulation of surface waves generated by a submarine landslide, equations (1.1), (1.2) considered in this paper are written in a quasi-conservative form, and in the case of flat bottom momentum balance equation (1.2) takes a totally conservative form. Another important feature of model (1.1), (1.2) is that it admits a total energy balance law [13] correlated with the similar law for three-dimensional equations, which confirms the physical consistency of this model and allows us to perform additional verification of calculations. Moreover, equations (1.1), (1.2) have the same structure as gas dynamics equations and this allows us to use algorithms based on well-studied numerical methods of gas dynamics as this was done for classic shallow water equations approximated by a finite difference predictor–corrector scheme [29, 42], or the MacCormack scheme on a uniform rectangular grid [39].

In this paper we reduce the numerical algorithm solving complicated system of NLD-equations (1.1), (1.2) containing mixed derivatives of velocity vector components to successive solution of two simpler problems at each time step. The first problem is to determine φ from the equation [21]:

$$\nabla \cdot \left(\frac{\nabla\varphi}{H} - \frac{(\nabla\varphi \cdot \nabla h)\nabla h}{Hr}\right) - 6\varphi\left(\frac{2}{H^3}\,\frac{r-3}{r} + \nabla \cdot \left(\frac{\nabla h}{H^2 r}\right)\right) = F \tag{1.3}$$

where

$$F = \nabla \cdot \left(g\nabla\eta + \frac{R\nabla h}{r}\right) - \frac{6R}{Hr} + 2(\nabla \cdot \boldsymbol{u})^2 - 2(u_x v_y - u_y v_x).$$

This is a uniformly elliptic equation, it does not contain time derivatives for the velocity vector components and under some restrictions [19] on $|\nabla h|$ it can be approximated by a difference scheme with a selfadjoint positive definite operator, which guarantees the convergence of iterative methods.

The second problem is to solve the system of hyperbolic type consisting of continuity equation (1.1) and equation (1.2) rewritten in the form of a motion equation in the dispersion free shallow water model with a modified right-hand side, i.e.,

$$(H\boldsymbol{u})_t + \nabla \cdot (H\boldsymbol{u}\boldsymbol{u}) + \nabla\frac{gH^2}{2} = gH\nabla h + \nabla\varphi - \frac{\nabla h}{r}\left(\frac{6\varphi}{H} + HR + \nabla\varphi \cdot \nabla h\right). \tag{1.4}$$

The decomposition of original system (1.1), (1.2) into two more simple problems allows us to solve NLD-equations numerically using the algorithm of NLSW-model [20, 40] modified so that the problem for equation (1.3) is additionally solved at each step of the predictor–corrector scheme.

We assume that in the plane $z = 0$ the contour of the water area is contained in a certain rectangle covered by a uniform rectangular grid, the shore line is approximated by a polyline Γ whose segments go along coordinate lines of the grid. The no-penetration condition $\boldsymbol{u} \cdot \boldsymbol{n}|_\Gamma = 0$ is posed on the line Γ, where $\boldsymbol{n}$ is the vector of the outer normal to the corresponding segment of the polyline Γ. We also suppose that the bottom is fixed near the shore. In order to simplify the boundary conditions, we align the bottom in a neighbourhood of the shore line so that if the depth is less than a certain given value h_w, it is set equal to h_w. In this case the boundary condition for the function φ on a rectilinear part of the boundary Γ takes the form

$$\frac{\partial \varphi}{\partial n} - gH\frac{\partial \eta}{\partial n} = 0.$$

We suppose the water is at rest at the initial time moment ($\eta \equiv 0$, $\boldsymbol{u} \equiv \boldsymbol{0}$).

2 Submarine landslide model

Concerning the choice of the landslide model, the evident lack of information on physical characteristics of its motion along underwater paths leads us to conclusion to use simplified models. We consider one of such models. We represent the function $z = -h(x, y, t)$ as a sum of two functions, the first one $z = h_0(x, y) < 0$ specifies the fixed bottom and the second $z = h_s(x, y, t) \geq 0$ determines the upper border of the moving landslide. The model of landslide motion used here is based on the assumption that at each time moment the position of the landslide is determined by the point $\boldsymbol{x}_c(t) = \big(x_c(t), y_c(t), z_c(t)\big)$ sliding over the bottom according to the law of non-free motion of a material point along a curvilinear surface. The connection between the positions of the landslide and the point $\boldsymbol{x}_c(t)$ means that if at the initial time moment $t = 0$ the landslide is at rest, the function $z = h_s^0(x, y)$ with a finite support $\mathcal{D}_0$ specifies its initial form, and the point $\boldsymbol{x}_c(0)$ has the coordinates $x_c(0) = x_c^0$, $y_c(0) = y_c^0$, $z_c(0) = z_c^0 = h_0\left(x_c^0, y_c^0\right)$, and $\left(x_c^0, y_c^0\right) \in \mathcal{D}_0$, then for $t > 0$ the landslide surface is given by the function $h_s(x, y, t) = h_s^0(x + x_c^0 - x_c(t),\ y + y_c^0 - y_c(t))$, whose support is the set

$$\mathcal{D}_t = \left\{(x, y) \mid (x + x_c^0 - x_c(t),\ y + y_c^0 - y_c(t)) \in \mathcal{D}_0\right\}.$$

According to these assumptions, the surface of the landslide moving along a curvilinear slope will be deformed and thus we can say that the model of a real landslide is that of a quasi-deformable body.

The forces determining the landslide motion are the forces of gravity, buoyancy, friction on the bottom, and water resistance. The calculation of the first three forces takes into account the form of landslide and its position on the slope. The force of water resistance is calculated according to the maximal area of landslide cross-section by a vertical plane perpendicular to the horizontal component of the velocity vector at the center of mass. The equations for landslide motion subject to assumptions presented above were obtained in [3], these equations include the following parameters: the landslide volume V; the coefficients of associated mass C_w, friction C_{fr}, and hydrodynamic resistance C_d; $\gamma = \rho_s/\rho_w > 1$, where ρ_w is the water density and ρ_s is the density of landslide mass; $C_{fr} = \tan \vartheta_\star$, $\vartheta_\star$ is the angle of friction. Motion equations are solved until the moment of landslide stop.

The working ability of the calculation algorithm was confirmed for model water areas [6, 8, 20, 21, 40, 41] by a good correspondence of the results obtained with its use within the NLD-model with the known experimental results of the laboratory of simulation of landslide processes and the calculation results obtained with the mathematical model of potential flows of an incompressible fluid with a free boundary in the two-dimensional [26] and three-dimensional [27] approximations. A parametric analysis of the landslide mechanism of surface wave generation was performed [3, 7, 28] with the use of this algorithm by variation of such parameters as the initial depth of the model landslide, its side and density, the coefficients of associated mass, friction, hydrodynamic resistance, the steepness and curvature of underwater slopes of simple geometry (flat ones, or given by analytic functions).

Using the model of a quasi-deformable landslide, we carried out a study of characteristics of the actual tsunami appearing in the water area near the coast of Papua New Guinea on July 17, 1998. It is known [2, 16, 45]

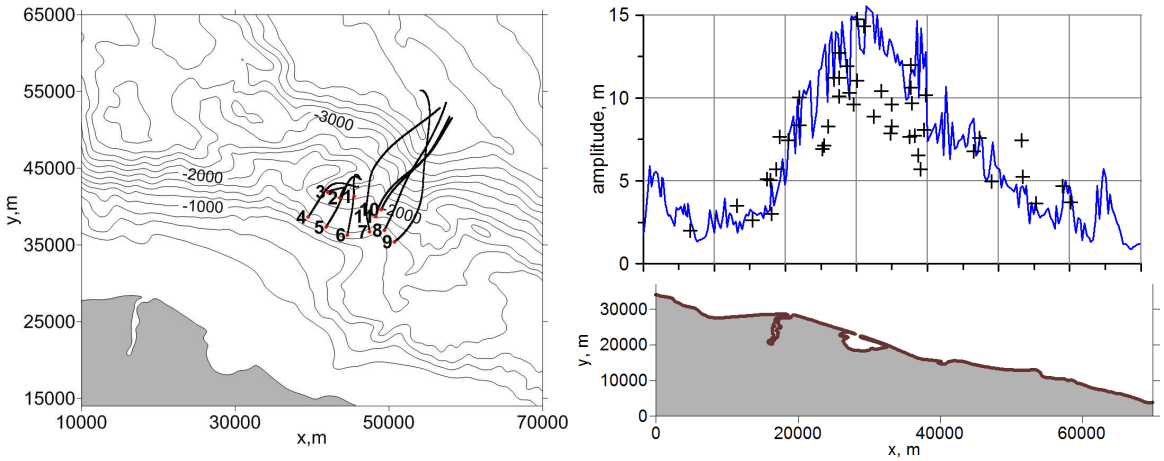

(a) (b)

Figure 1. (a) Motion trajectories of the landslide center of mass for its different initial positions; (b) calculated distribution (solid line) of maximal wave heights along the shore line, tsunami wave heights most correlated to field measurements (markers).

that this event was related to a large submarine landslide. It was studied well and thoroughly documented. The main goal of simulation was the determination of the possible initial position of the landslide material on the underwater slope. We considered 11 variants of initial positions including the variants quite different from commonly accepted. The physical parameters of the landslide model were taken close to those used in [45]. The initial form of the model landslide was specified by the formula

$$h_s^0(x,y) = \begin{cases} \dfrac{T}{4}\left[1+\cos\left(\dfrac{2\pi(x-x_c^0)}{b_1}\right)\right]\cdot\left[1+\cos\left(\dfrac{2\pi(y-y_c^0)}{b_2}\right)\right], & (x,y)\in\mathcal{D}_0 \\ 0, & (x,y)\notin\mathcal{D}_0 \end{cases} \tag{2.1}$$

where $\mathcal{D}_0 = \left[x_c^0 - b_1/2,\ x_c^0 + b_1/2\right]\times\left[y_c^0 - b_2/2,\ y_c^0 + b_2/2\right]$, b_1 and b_2 are the lengths of the landslide along the axes Ox and Oy, respectively, x_c^0 and y_c^0 are the given abscissa and ordinate of its center of mass, T is the thickness.

The simulation was performed within the classic nonlinear shallow water equations with the use of the finite-difference MacCormack scheme [39] on a uniform grid with the spatial mesh size of 100 m constructed on the base of the digital World ocean relief of GEBCO. The use of a dispersion free NLSW-model is in accordance with the results of [35] indicating that for the event considered in this case the dispersion has no essential influence on the process of wave propagation in a coastal zone.

Figure 1a presents the calculated trajectories of the motion of the landslide center of mass for its different initial positions. As is seen from the figure, the landslide may stop directly on the slope in a small cavity or 'amphitheater' at the depth about 2500 m (trajectories 1–6) as well as continue its movement until the abyss of the water area (trajectories 7–11). The results most close to the observed ones were obtained for the landslide positioned at the initial time moment at the points 5 and 6.

After that we performed updating calculations where the initial positions of landslide were taken in a neighbourhood of these two points and its parameters were specified according to the choice of the authors of [23], in particular, we assumed that $b_1 = 3000$ m, $b_2 = 5000$ m, $T = 450$ m, $\vartheta_\star = 12^\circ$. Figure 1b shows the distribution of the maximal wave heights along the shore line for the variant providing the best correspondence to the field data [44] for the event occurring in 1998. The comparison of the obtained results with the field data and also with the calculation results of other authors [23, 44] gives us the confidence that our landslide model is adequate and the conjecture on localization of the initial landslide position is justified.

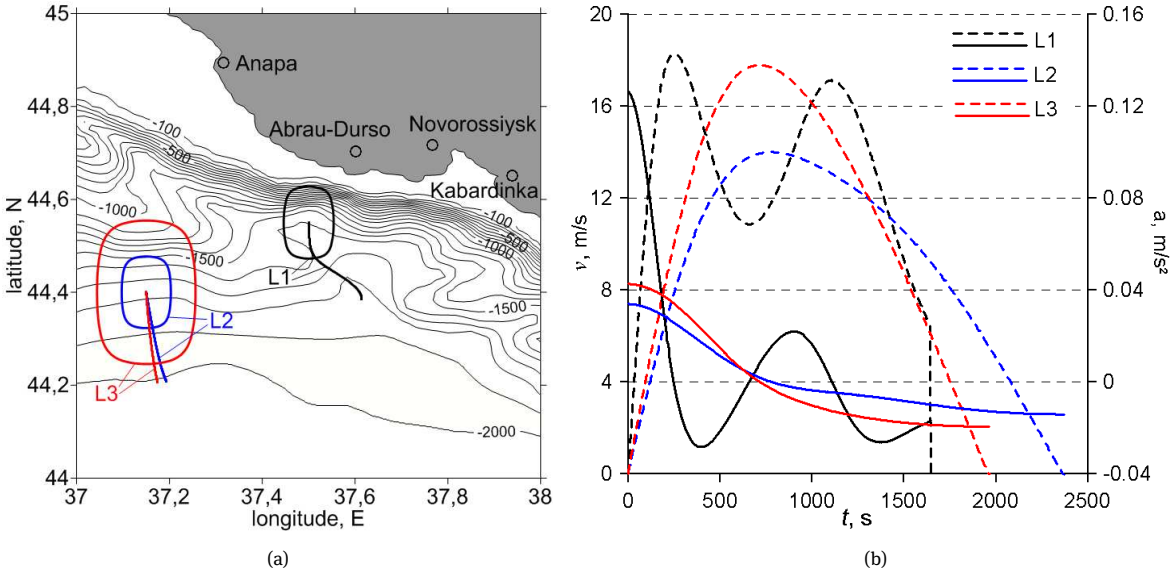

Figure 2. (a) Draft fragment of the computation water area with drawn isolines of bottom relief, contours of model landslides, and trajectories of their motion; (b) graph of velocities v (dotted lines) and accelerations a (solid lines) of centers of mass of model landslides.

3 Some results of simulation of tsunami waves generated by landslides in the Black Sea

The main goal of numerical experiments whose results are presented in this section was to determine the peculiarities of wave modes in the near and far zones of the water area under different initial positions of landslide and to evaluate the parameters affecting its motion, we also estimated the influence of the dispersion on the wave field. Due to strict restrictions on the size of this paper, we present here only some results for model landslides positioned initially at the foot of the continental slope near the site of the historic landslide [25], having the volume $V_0 = 40$ km^3, the thickness $T_0 = 200$ m, and the base area $S_0 = 200$ km^2.

The initial position of the three model landslides L1, L2, and L3 having the same thickness $T = T_0$ are schematically shown in Fig. 2a by contours of different color. For $t = 0$ the landslides L2 and L3 have approximately the same coordinates of the center of mass (37.15°E, 44.4°N) and depth $z_c^0 = -1769$ m as the historic landslide, but differ from it in volume and area. These distinctions are caused by the need to provide sufficient smoothness of the surface of the model landslide required for calculations within the NLD-model and given by formula (2.1) according to which we have $V = Tb_1b_2/4 = TS/4$. Therefore, the model landslide L2 has the same area $S = S_0$ as the historic one, but its volume is a quarter. For the landslide L3 with the area $S = 4S_0$ we have the equality of volumes $V = V_0$. The landslide L1 with the coordinates of the center of mass (37.5°E, 44.55°N) had the same sizes as L2, but was located higher on the slope ($z_c^0 = -1598$ m) at the initial time moment.

Figure 2a also shows the trajectories of landslide motion for the following values of the parameters: $C_w = 1$, $C_d = 1$, $\gamma = 2$. The values of the friction angle $\vartheta_\star$ were taken so that the model landslides passes over the slope the same distance as the historic one (approximately 22 km [25]). Since the landslides L2 and L3 were located on a gentle (practically flat) foot of the continental slope, their trajectories occur to be close to rectilinear ones. The long bottom deformation generates waves of small amplitude. This deformation leads to a small increase of velocity and smooth stopping of the landslides L2 and L3 (see Fig. 2b where the left vertical axis of the coordinate system corresponds to the absolute value of the velocity vector $v = |\boldsymbol{v}|$ and the right one corresponds to the value $a = \mathrm{d}v/\mathrm{d}t$).

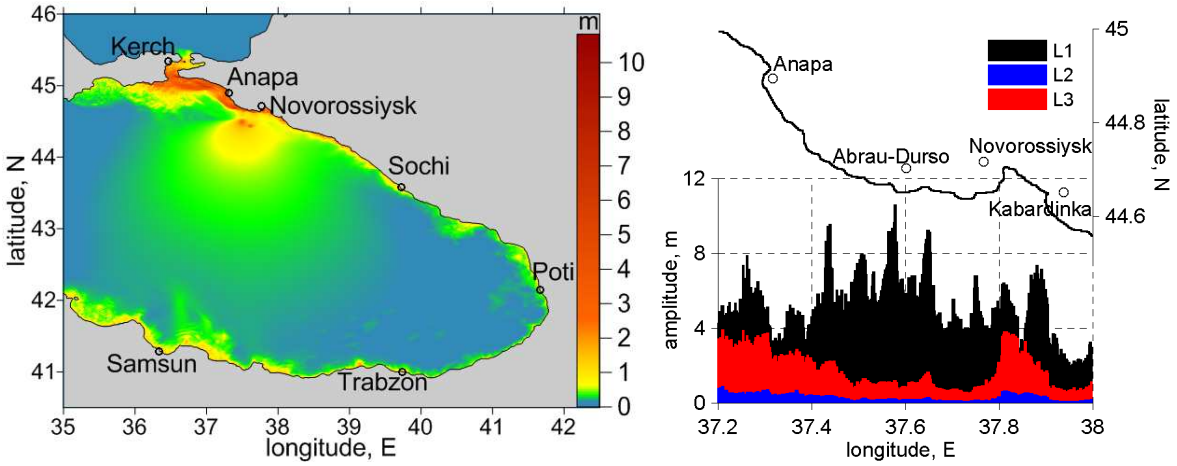

Figure 3. (a) Distributions of maximal amplitudes of tsunami waves generated by the model landslide L1 and calculated for the 3rd hour of physical time of their propagation; (b) distribution of maximal wave heights along a part of the shore line. NLD-model.

At the beginning of landslide motion a positive crescent-shaped wave appears near it and this wave spreads with formation of a lowering wave at back front. A 'hollow' is formed above the landslide, it accompanies the landslide and gradually disappears as the landslide moves into the deep zone of the water area. With time, the lowering wave arising here begins to spread in the direction opposite to the direction of landslide movement (into the shallow coastal water area) and after its reflection from the shore it goes to deep water in the form of a positive wave. In this case, a landslide of greater volume, under equal other conditions, generates higher waves on the shore (see Fig. 3b).

More dangerous waves appear in the motion of the landslide L1. Its upper part is initially positioned at a rather steep part of the slope and hence it attains the velocity 18 m/s with a greater acceleration (for the chosen value of $\vartheta_\star = 0.8^\circ$) and, falling into the underwater canyon, it has sharply turned two times and stopped abruptly at the end of its path. Such sharp stop leads to appearance of a new element of the wave field, namely, a considerable positive wave with large amplitudes on the shore horizon. Such effect was indicated previously (see, e.g., [6, 41]) in model water areas of simple geometry. The curvilinear motion trajectory of the landslide L1 complicates the interaction of waves generated by it and large initial accelerations become the origin of considerable amplitudes along the shore line. We note that the maximal values of those amplitudes are attained not at the coastal point closest to the landslide position, but at the place where the leading crescent-shaped wave comes to the shore. The distribution of maximal wave elevations on the shore is extremely irregular (see Fig. 3b) and it strongly depends on the extent of the shelf zone, coastal bathymetry, and shore line geometry. In the case of the landslide L1, the most vulnerable parts of the coast are located at a short distance from the center of landslide, which can be seen from Figure 3a showing the distribution of the maximal amplitudes in the eastern part of the water area in the time of calculation and indicating, in particular, the absence of the radial symmetry in propagation of the wave energy whose main portion is directed towards the northern fragment of the Russian coast.

We note that the results presented above were obtained on a uniform rectangular grid covering the water areas of the Black and Azov seas from 27°E to 42.5°E and from 40.5°N to 47.5°N. Preliminary calculations we performed on a coarse grid constructed on the base of 'The GEBCO One Minute Grid - 2008' digital relief. After that the results were recalculated on a refined grid with the mesh sizes $h_x = 333.28$ m, $h_y = 463.32$ m in the directions of the Cartesian axes Ox and Oy and, finally, on the finest grid with half-sized steps $h_x = 166.64$ m, $h_y = 231.66$ m. The comparison of the results calculated on these three grids at the points of location of virtual deep sea tide gauges have shown that for the first few waves we have the convergence. However, a detailed reproduction of the interaction between waves and the shore (a vertical wall installed at the depth of

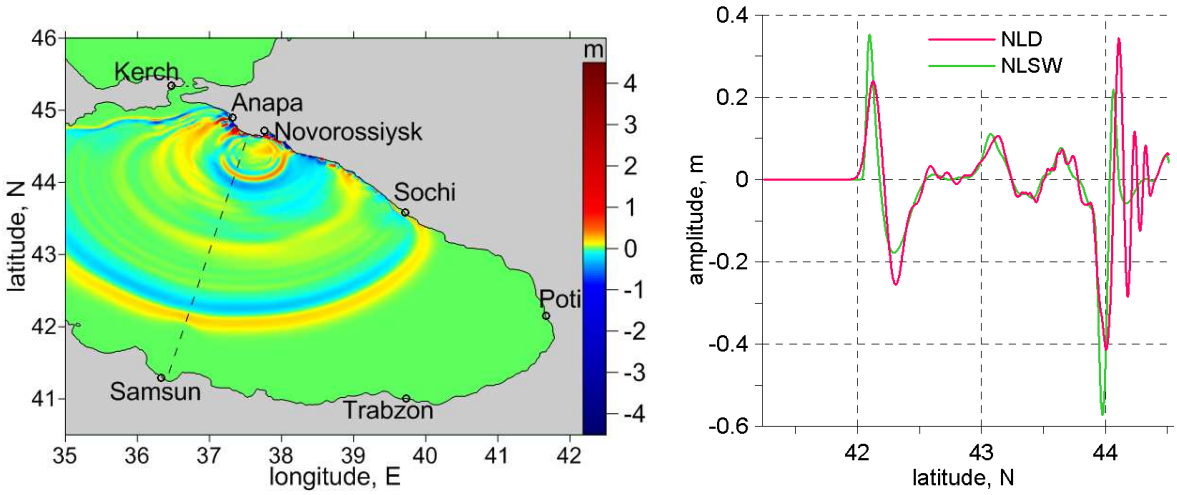

Figure 4. (a) Free surface calculated by the NLD-model; (b) sections of free surfaces. Landslide L1; $t = 2000$ s.

$h_w = 20$ m) requires computations on grids with even greater resolution because the refining of grid reveals subgrid details of the bathymetry and coastline which cannot be reproduced on coarse grids, but strongly affect the dynamics of short waves in the coastal zone. One of the techniques capable of providing a sufficient computation accuracy is the use of telescopically nested grids in a neighbourhood of the most important parts of the coast [22].

A general view of the dynamics of the wave modes generated by a landslide can be obtained with an appropriate choice of the sequence of free surface filed pictures calculated at different time moments. One of such pictures is presented in Fig. 4a with the use of a color scale indicating the deviation of the water level from its unperturbed state. As is seen from the picture, after 33 minutes from the beginning of landslide movement the dominant elements of the wave field are the leading wave and two waves reflected from the shore. As the distance from the source of perturbation increases, the amplitudes of these waves decrease, but they begin to grow when the waves go into wide parts of the southern shelf and may reach two meters at the shore line (see Fig. 3a). We should also point out the deformation of wave fronts caused by unevenness of distributions of their motion velocities in the water area with a strongly uneven distribution of depths.

In order to estimate the influence of the dispersion on the process of wave propagation, we considered sections of free surface distributions calculated at different time moments. The comparison of the calculations results obtained from NLD- and NLSW-models has shown that within this range of problems the dispersion weakly affects wave fields at the initial stage of the process and also in the interaction of waves with parts of the coast close to the initial position of the landslide. The time of the first wave arrival to these parts occurred to be small and hence dispersive effects cannot become apparent. The landslides L2 and L3 generate so long waves that dispersive effects have no influence during the entire process. The dispersion of waves generated by the landslide L1 is more visible.

Figure 4a shows the position of the section passing through the point of initial position of the center of mass of the landslide L1 and directed to the Samsun city (Turkey). To the time corresponding to Fig. 4a, the leading wave has passed the largest part of its path to the southern coast leaving behind a dispersive tale of short waves of small amplitude. The dispersion is more clear after appearance of the wave ($t \approx 1700$ s) caused by the abrupt stop of the landslide. This wave has steep slopes and breaks down into a series of short waves clearly visible in the right-hand side of Fig. 4b. The dispersion free NLSW-model does not reproduce such feature of the wave field.

We have to note an important role of the extensive shallow shelf adjacent to some parts of the southern coast of the Black Sea, which filters out short-wave dispersion waves appearing in the deep water areas. As the result, some tide gauges close to the shore indicate a good correlation of the results obtained from NLD-

and NLSW-models. The mareograms calculated at most remote points of the water area are slightly different, but these differences are not so essential as to speak of primary importance of the dispersion in formation of the wave field near the southern coast.

More noticeable differences occur in the deep part of the water area. In particular, the amplitude of the leading wave calculated using the NLD-model is significantly less than that determined by the NLSW-model, and it propagates with a lesser velocity. In addition, in a long propagation process the maximum of the amplitude may drift to the dispersive tail (see also [16, 33, 34]).

4 Conclusion

A numerical technique for the study of surface waves appearing in the event of submarine landslide is proposed. The technique is based on the simultaneous use of the model of motion of a quasi-deformable body over a curvilinear surface [3] and the total nonlinear dispersive shallow water model taking into account the bottom movement and derived without assumptions on the potential character of the flow and small wave amplitudes [13]. The technique allows us to perform scenario calculations of problems close to real ones with varying the parameters affecting the motion of landslide and also obtain a detailed wave picture on the stages of wave generation, their spread over the water area, and interaction with near and far coastal zones.

The detailed analysis of wave fields calculated in numerical experiments has led us to several important conclusions. In particular, it was shown that dispersive effects are clearly pronounced for more compact landslides and for greater values of their initial acceleration. The influence of the dispersion essentially weakens when waves go on extended shallow zones of real water areas. The use of shallow water models of the first approximation leads to overestimated amplitudes of spreading waves.

In this paper we does not take into account the effects related to the sphericity and rotation of the Earth, which is explained by a small size of the Black Sea water area. Certainly, such effects and the dispersion of waves should be taken into account for large water areas, as this was done, e.g., in [30] where a weakly dispersive shallow water model was used for calculations. The authors of this paper plan to carry out similar researches with the use of a more accurate model, i.e., the total nonlinear dispersive model on a rotating sphere [12].

Funding: The work was supported by the Russian Scientific Foundation (project No. 14–17–00219).

References

[1] S. Assier-Rzadkiewicz, P. Heinrich, P. C. Sabatier, B. Savoye, and J. F. Bourillet, Numerical modelling of a landslide-generated tsunami: the 1979 Nice event. *Pure Appl. Geophys.* **157** (2000), 1707–1727.

[2] J. P. Bardet, C. E. Synolakis, H. L. Davies, F. Imamura, and E. A. Okal, Landslide tsunamis: recent findings and research directions. *Pure Appl. Geophys.* **160** (2003), 1793–1809.

[3] S. A. Beisel, L. B. Chubarov, D. Dutykh, G. S. Khakimzyanov, and N. Yu. Shokina, Simulation of surface waves generated by an underwater landslide in a bounded reservoir. *Russ. J. Numer. Anal. Math. Modelling* **27** (2012), No. 6, 539–558.

[4] S. A. Beisel, L. B. Chubarov, and G. S. Khakimzyanov, Simulation of surface waves generated by an underwater landslide moving over an uneven slope. *Russ. J. Numer. Anal. Math. Modelling* **26** (2011), No. 1, 17–38.

[5] M. J. Castro, M. de la Asuncion, J. Macias, C. Pares, E. D. Fernandez-Nieto, J. M. Gonzalez-Vida, and T. Morales, IFCP Riemann solver: application to tsunami modelling using GPUs. In: *Numerical Methods for Hyperbolic Equations: Theory and Applications. Int. Conf. to Honour Prof. E. F. Toro.* CRC Press, 2013, pp. 237–244.

[6] L. B. Chubarov, S. V. Eletskii, Z. I. Fedotova, and G. S. Khakimzyanov, Simulation of surface waves generation by an underwater landslide. *Russ. J. Numer. Anal. Math. Modelling* **20** (2005), No. 5, 425–437.

[7] L. B. Chubarov, G. S. Khakimzyanov, and N. Yu. Shokina, Numerical modelling of surface water waves arising due to movement of underwater landslide on irregular bottom slope. In: *Notes on Numerical Fluid Mechanics and Multidisciplinary Design. Computational Science and High Performance Computing IV*, Vol. 115, Springer-Verlag, Berlin, Heidelberg, 2011, pp. 75–91.

[8] S. V. Eletskii, Yu. B. Maiorov, V. V. Maksimov, I. S. Nudner, Z. I. Fedotova, M. G. Khazhoyan, G. S. Khakimzyanov, and L. B. Chubarov, Simulation of surface waves generation by a moving part of the bottom down the coastal slope. *Comp. Tech.* **9** (2004), Part 2, 194–206 (in Russian).

[9] F. Enet and S. T. Grilli, Experimental study of tsunami generation by three-dimensional rigid underwater landslides. *J. Waterway Port Coastal Ocean Engrg.* **133** (2007), No. 6, 442–454.

[10] Yu. D. Evsyukov, Distribution of landslide bodies on the continental slope of the north-eastern part of the Black Sea. *Izv. North Caucasus Scientific Centre of the Higher School. Natural Sci.* **6** (2009), 100–104 (in Russian).

[11] Z. I. Fedotova and G. S. Khakimzyanov, Shallow water equations on a movable bottom. *Russ. J. Numer. Anal. Math. Modelling* **24** (2009), No. 1, 31–41.

[12] Z. I. Fedotova and G. S. Khakimzyanov, Nonlinear-dispersive shallow water equations on a rotating sphere. *Russ. J. Numer. Anal. Math. Modelling* **25** (2010), No. 1, 15–26.

[13] Z. I. Fedotova, G. S. Khakimzyanov, and D. Dutykh, On the energy equation of approximate models in the long-wave hydrodynamics. *Russ. J. Numer. Anal. Math. Modelling* **29** (2014), No. 3, 167–178.

[14] E. D. Fernandez-Nieto, F. Bouchut, D. Bresh, M. J. Castro, and A. Mangeney, A new Savage-Hutter type model for submarine avalanches and generated tsunami. *J. Comput. Phys.* **227** (2008), No. 16, 7720–7754.

[15] I. A. Garagash, L. I. Lobkovskii, O. R. Kozyrev, and R. Kh. Mazova, Generation and run-up of tsunami waves caused by a submarine landslide. *Oceanology* **43** (2003), No. 2, 153–161.

[16] S. Glimsdal, G. K. Pedersen, C. B. Harbitz, and F. Lovholt, Dispersion of tsunamis: does it really matter? *Nat. Hazards Earth Syst. Sci.* **13** (2013), 1507–1526.

[17] S. T. Grilli, S. Vogelmann, and P. Watts, Development of a 3D numerical wave tank for modelling tsunami generation by underwater landslides. *Engrg. Anal. Boundary Elements* **26** (2002), 301–313.

[18] S. T. Grilli and P. Watts, Tsunami generation by submarine mass failure. I : Modelling, experimental validation, and sensitivity analyses. *J. Waterway Port Coastal Ocean Engrg.* **131** (2005), No. 6, 283–297.

[19] O. I. Gusev, On an algorithm for surface waves calculation within the framework of nonlinear dispersive model with a movable bottom. *Comp. Tech.* **17** (2012), No. 5, 46–64 (in Russian).

[20] O. I. Gusev, Algorithm for surface waves calculation above a movable bottom within the frame of plane nonlinear dispersive model. *Comp. Tech.* **19** (2014), No. 6, 19–41 (in Russian).

[21] O. I. Gusev, N. Yu. Shokina, V. A. Kutergin, and G. S. Khakimzyanov, Numerical modelling of surface waves generated by underwater landslide in a reservoir. *Comp. Tech.* **18** (2013), No. 5, 74–90 (in Russian).

[22] V. K. Gusyakov, Z. I. Fedotova, G. S. Khakimzyanov, L. B. Chubarov, and Yu. I. Shokin, Some approaches to local modelling of tsunami wave runup on a coast. *Russ. J. Numer. Anal. Math. Modelling* **23** (2008), No. 6. 551–565.

[23] P. Heinrich, A. Piatanesi, and H. Hebert, Numerical modelling of tsunami generation and propagation from submarine slumps: the 1998 Papua New Guinea event. *Geophys. J. Intern.* **145** (2001), 97–111.

[24] M. Ioualalen, S. Migeon, and O. Sardoux, Landslide tsunami vulnerability in the Ligurian Sea: case study of the 1979 October 16 Nice international airport submarine landslide and of identified geological mass failures. *Geophys. J. Intern.* **181** (2010), 724–740.

[25] R. A. Kazantsev and V. V. Kruglyakov, Giant landslide on the Black Sea floor. *Priroda* **10** (1998), 86–87 (in Russian).

[26] G. S. Khakimzyanov and M. G. Khazhoyan, Numerical simulation of the interaction between surface waves and submerged obstacles. *Russ. J. Numer. Anal. Math. Modelling* **19** (2004), No. 1, 17–34.

[27] G. S. Khakimzyanov and Yu. I. Shokin, A finite-difference method for calculating surface waves in coastal zone. *Russ. J. Numer. Anal. Math. Modelling* **8** (1993), No. 6, 461–481.

[28] G. S. Khakimzyanov and N. Yu. Shokina, Evaluation of the height of waves generated by an underwater landslide in a confined water reservoir. *J. Appl. Mech. Tech. Phys.* **53** (2012), No. 5, 690–699.

[29] G. S. Khakimzyanov and N. Yu. Shokina, Adaptive grid method for one-dimensional shallow water equations. *Comp. Tech.* **18** (2013), No. 3, 54–79 (in Russian).

[30] J. T. Kirby, F. Shi, B. Tehranirad, J. C. Harris, and S. T. Grilli, Dispersive tsunami waves in the ocean: Model equations and sensitivity to dispersion and Coriolis effects. *Ocean Modelling* **62** (2013), 39–55.

[31] E. K. Lindstrom, G. K. Pedersen, A. Jensen, and S. Glimsdal, Experiments on slide generated waves in a 1:500 scale fjord model. *Coastal Engrg.* **92** (2014), 12–23.

[32] P. L.-F. Liu, T.-R. Wu, F. Raichlen, C. E. Synolakis, and J. Borrero, Runup and rundown generated by three-dimensional sliding masses. *J. Fluid Mech.* **536** (2005), 107–144.

[33] F. Lovholt, G. Pedersen, and G. Gisler, Oceanic propagation of a potential tsunami from the La Palma Island. *J. Geophys. Res.* **113** (2008), C09026.

[34] F. Lovholt, G. Pedersen, and S. Glimsdal, Coupling of dispersive tsunami propagation and shallow water coastal response. *Open Oceanogr. J.* **4** (2010), 71–82.

[35] P. J. Lynett, J. C. Borrero, P. L.-F. Liu, and C. E. Synolakis, Field survey and numerical simulations: a review of the 1998 Papua New Guinea tsunami. *Pure Appl. Geophys.* **160** (2003), 2119–2146.

[36] P. J. Lynett and P. L.-F. Liu, A numerical study of submarine-landslide-generated waves and run-up. *Proc. R. Soc. A.* **458** (2002), 2885–2910.

[37] B. G. Pustovitenko and V. E. Kulchitskii, Seismicity of the Black Sea depression. *Geophys. J.* **13** (1991), No. 1, 14–19 (in Russian).
[38] B. Ranguelov, S. Tinti, G. Pagnoni, R. Tonini, F. Zaniboni, and A. Armigliato, The nonseismic tsunami observed in the Bulgarian Black Sea on 7 May 2007: was it due to a submarine landslide? *Geophys. Res. Letters* **35** (2008), L18613.
[39] Yu. I. Shokin, V. V. Babailov, S. A. Beisel, L. B. Chubarov, S. V. Eletskii, Z. I. Fedotova and V. K. Gusyakov, Mathematical modelling in application to regional tsunami warning systems operations. In: *Notes on Numerical Fluid Mechanics and Multidisciplinary Design. Computational Science and High Performance Computing III*, Vol. 101, Springer-Verlag, Berlin–Heidelberg, 2007, pp. 52–69.
[40] Yu. I. Shokin, S. A. Beisel, O. I. Gusev, G. S. Khakimzyanov, L. B. Chubarov, and N. Yu. Shokina, Numerical modelling of dispersive waves generated by landslide motion. *Bull. South Ural State Univ. Ser. 'Mathematical Modelling, Programming, Computer Software'* **7** (2014), No. 1, 121–133 (in Russian).
[41] Yu. I. Shokin, Z. I. Fedotova, G. S. Khakimzyanov, L. B. Chubarov, and S. A. Beisel, Modelling surfaces waves of generated by a moving landslide with allowance for vertical flow structure. *Russ. J. Numer. Anal. Math. Modelling* **22** (2007), No. 1, 63–85.
[42] N. Yu. Shokina, To the problem of construction of difference schemes on movable grids. *Russ. J. Numer. Anal. Math. Modelling* **27** (2012), No. 6, 603–626.
[43] O. N. Solov'eva, S. F. Dotsenko, I. P. Kuzin, and B. V. Levin, Tsunami in the Black Sea: historical events, seismic sources, and features of propagation. *Oceanology* **44** (2004), No. 5, 638–643.
[44] C. E. Synolakis, J.-P. Bardet, J. C. Borrero, H. L. Davies, E. A. Okal, E. A. Silver, S. Sweet, and D. R. Tappin, The slump origin of the 1998 Papua New Guinea tsunami. *Proc. R. Soc. A.* **458** (2002), 763–789.
[45] D. R. Tappin, P. Watts, and S. T. Grilli, The Papua New Guinea tsunami of 17 July 1998: anatomy of a catastrophic event. *Natural Hazards Earth System Sci.* **8** (2008), 243–266.
[46] S. Tinti, E. Bortolucci, and C. Vannini, A block-based theoretical model suited to gravitational sliding. *Natural Hazards* **16** (1997), 1–28.
[47] P. Watts, S. T. Grilli, J. T. Kirby, G. J. Fryer, and D. R. Tappin, Landslide tsunami case studies using a Boussinesq model and a fully nonlinear tsunami generation model. *Natural Hazards Earth System Sci.* **3** (2003), No. 5, 391–402.
[48] P. Watts, F. Imamura, and S. T. Grilli, Comparing model simulations of three benchmark tsunami generation cases. *Sci. Tsunami Hazards* **18** (2000), No. 2, 107–123.
[49] A. Yalciner, E. Pelinovsky, T. Talipova, A. Kurkin, A. Kozelkov, and A. Zaitsev, Tsunamis in the Black Sea: comparison of the historical, instrumental and numerical data. *J. Geophys. Research* **109** (2004), No. C12023.